JOURNAL OF MATERIALS SCIENCE 13 (1978) 833–842

Microhardness in PbTe and related alloys

A. J. CROCKER, M. WILSON
School of Materials Science and Physics, Thames Polytechnic, London, UK

The microhardness of PbTe has been determined as a function of applied load. Work hardening is found to occur with the hardness increasing as the square root of the applied load. The effect of holes for $p > 10^{18}$ cm^{-3} is to increase the hardness but no similar effect is found for free electrons. A possible explanation is offered in terms of electrostatic interaction between dislocations and charged impurities. For constant hole concentrations, alloying with SnTe softens PbTe and alloying with CdTe hardens PbTe.

1. Introduction

A considerable literature exists on the electrical and physico-chemical properties of the IV–VI group of semiconductors. Many devices have been made from these materials from thermoelectric elements to infra-red detectors. Currently, much interest is being shown and much effort expended in making detectors from these materials to work in the 8 to 14 μm region of the infra-red spectrum. During the fabrication of these devices it is necessary to have very careful mechanical handling techniques since it is extremely easy to introduce work damage into the specimens. This work damage may be deleterious to the performance of p–n junctions subsequently formed for infra-red detection. The material is so soft that a paper tissue dragged across the surface of the specimen leaves behind a trail of dislocations. Damage introduced into the specimen by sawing can be extensive, up to a few hundred microns in depth. Although dislocations are easily introduced the material is not very ductile i.e. dislocations are easily induced but are not particularly mobile.

Various authors have investigated the hardness of PbTe, by compressive loading [1] or indentation [2], as a function of carrier concentration and impurity content. The high susceptibility of PbTe and $Pb_{1-x}Sn_xTe$ to very small stresses and at the same time not behaving very plastically at higher stresses suggested that some work hardening may be occurring. In this investigation, hardness was therefore measured as a function of stress.

The energy gap of PbTe can be increased by alloying with CdTe [3] or decreased by alloying with SnTe [4]. In order to maximize the responsivity of an infra-red detector it is necessary to adjust the energy gap of the semiconductor close to the energy of the radiation to be detected. In the case of PbTe, SnTe is alloyed to reduce the energy gap to a suitable value e.g. for 10.6 μm detection an alloy of 20% SnTe can be used. A series of $Pb_{1-x}Sn_xTe$ and $Pb_{1-y}Cd_yTe$ alloy samples containing x and y up to 0.03 were measured in order to determine if, associated with this change in energy gap, there was a change in hardness.

2. Surface preparation

The crystals used in this investigation were grown by the Bridgman–Stockbarger method from tellurium-rich melts of composition $M_1\ Te_{1.005}$ where M is the total metal concentration. All investigations were carried out on room temperature freshly cleaved (1 0 0) cleavage planes of single crystal samples approximately 3 mm x 3 mm x 3 mm. The samples were mounted onto glass slides with a low melting point wax with the cleaved face parallel to the slide surface. The cleaved surfaces were chemically polished for several minutes in a solution consisting of 100 parts concentrated hydrobromic acid and 6 parts bromine at room temperature. The etch used for revealing the dislocations (Coates etch [5]) consisted of 20 parts saturated potassium hydroxide solution, 2 parts glycerol and 1 part hydrogen peroxide.

Polishing and etching were carried out with continuous agitation of the sample followed by

immediate washing. In 1 min the chemical polish removed a layer approximately 20 μm thick. Great care was taken to ensure that the minimum amount of wax was used to mount the samples and that the face to be polished was quite clean.

After cleaving and mounting the samples were polished and etched until no work damage was present. The dislocation density was found to be 10^5 to 10^6 cm^{-2}. That etch pits are due to dislocations can be inferred from the fact that freshly cleaved specimens of lead telluride, after etching with Coates etch, have etch pit patterns which are the mirror image of each other. In addition the number of etch pits per unit length along the branches of a triple low angle grain boundary algebraically add up to unity. Although this may mean that only certain types of dislocations, e.g. pure edge, or only cetain orientations are being revealed, at least etch pits are an indication of the presence of these dislocations.

3. Microhardness measurements

In order to study the mechanical property of a solid one needs to study the processes of dislocation motion and the stress relationships involved. However, this is difficult to do and is not necessarily related to the type of damage which may be introduced into a slice during device fabrication.

In order to measure the resistance of the material to applied local stresses (as for example one might induce by picking up a slice with tweezers) the microhardness of the specimens was measured. One of the major problems with microhardness measurements is the difficulty of correlating results with more fundamental measurements on dislocation movement. For example, the strain rate is unknown and may differ markedly during the impression of the diamond into the material, e.g. the initial strain rate when the diamond first penetrates the material may be very much higher than when the diamond is fully impressed. Also the stress may change markedly during the diamond impression with a consequent change in dislocation velocity [11]. This makes analysis of the results in terms of multiplication, velocities and mobile fractions difficult. However, the measurement does correspond to the mechanical stresses that the material is subjected to during handling and has the advantage of experimental simplicity and hence has been used by previous investigators to study the hardness of the lead chalcogenides.

Point loading of the prepared specimens was carried out by means of the microhardness attachment on a Vickers projection microscope using a diamond indentor. The apex of the pyramidal indentor was pointed, the ridge length given as 0 μm.

The loads varied from 1 to 50 g and the microhardness value was taken as the average of several impressions made, with both diagonals being measured. The apparatus was balanced for each sample to ensure the correct load was applied.

It is difficult when making micohardness measurements on the Vickers microscope to ensure that the diamond is being impressed into the surface at a constant rate since the sample is being loaded manually. In this investigation, every effort was made to keep the rate of descent constant by one person lowering the sample whilst an observer noted the rate of descent. The rate of descent was kept at approximately 8 μm sec^{-1}. Contact was maintained for 15 sec each time. The shape and quality of impressions were good and the accuracy in microhardness determination was ~5%. The room temperature remained constant at 20° C. The surface to be measured was chemically polished, etched and then hardness tested with the sides of the indentor parallel and at 45° to the sides of the etch pits. No change in hardness with illumination was detected.

4. Electrical measurements

The carrier concentration was determined from the Hall effect at room temperature. Although, for these two valence bands materials, the room temperature Hall coefficient gives an incorrect value for the hole concentration (it undervalues the heavy hole concentration) it serves as a comparative measurement. The van der Pauw [6] technique was employed so that discs of arbitrary shape could be used. When all the microhardness determinations had been made the samples were ground such that two opposite sides were flat and parallel. No change in Hall coefficient has been noticed in these materials with work damage [7], probably because the high static dielectric constant screens out the imperfections, hence it was felt that the carrier concentration determined from the ground samples was correct. This was confirmed by mobility measurements. Small

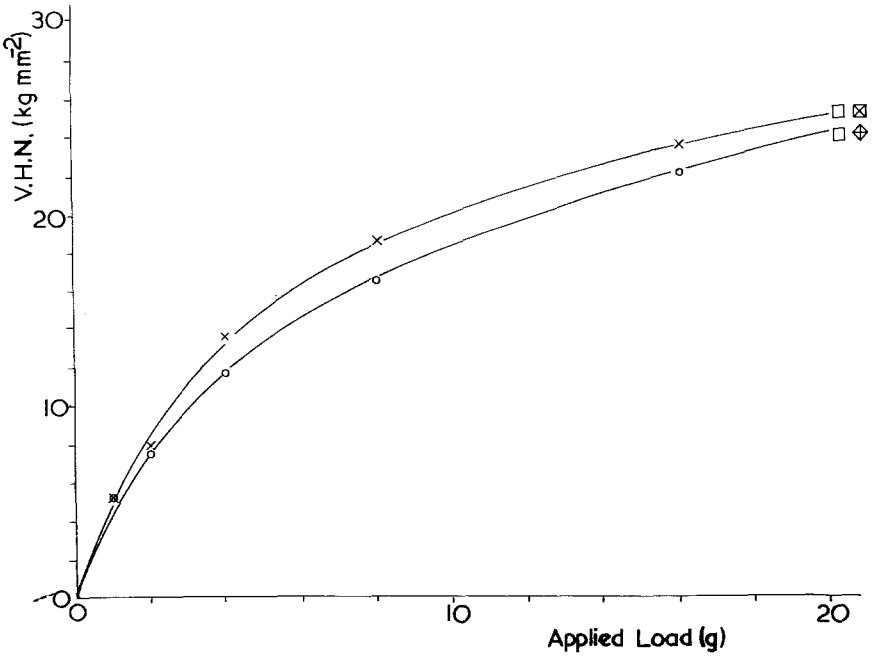

Figure 1 Variation of Vickers hardness number with applied load for non stoichiometric p-type PbTe ($p \sim 5 \times 10^{17}$ cm^{-3}). □ ⊠ sides of indentor parallel to etch pits, □ ⧫ sides of indentor at 45° to etch pits.

contacts were located at the circumference of the sample. The sample thickness was measured using a standard micrometer.

5. Investigations

5.1. Rosette structure

After the hardness measurements the surface was again Coates etched to reveal dislocations induced by the measurement. The size and surface shape of the dislocation patterns (rosettes) was investigated over a range of 1 to 50 g loads and at two orientations of the indentor. For each load the indentor was positioned with its sides parallel to, and at 45° to, the sides of the etch pits. Examination of the three-dimensional geometry was carried out on one specimen by successively removing the surface layer by chemical polishing and revealing the rosette pattern by etching.

5.2. Hardness

5.2.1. Undoped PbTe

Undoped PbTe need not be stoichiometric i.e. a crystal of undoped PbTe may contain an excess of lead or tellurium producing n- or p-type conduction respectively.

Production of stoichiometric crystals by the Bridgman–Stockbarger method is extremely difficult because the composition of the liquid phase for the lead chalcogenides does not remain constant. Consequently, crystals prepared by this method are inhomogeneous in their properties along the length of a crystal. The growth of PbTe from the stoichiometric melt produces initially a solid phase containing an excess of Te and having p-type conduction. As the melt solidifies the composition of the liquid phase gradually shifts to an increasing content of lead. This results in a corresponding change in the composition of the solid phase and may give rise to n-type conduction [14].

The undoped crystals used in this section exhibited p-type conduction and therefore contain a slight excess of tellurium atoms equivalent to approximately 5×10^{17} cm^{-3}. These samples were subjected to 2, 4, 6, 8, 10, 20, and in some cases 50 g loads. Fig. 1 shows the dependence of the hardness with increasing load. Rosette dimensions were measured for each load and Fig. 2 shows a similar dependence on applied load.

5.2.2. Doped and alloyed PbTe

In these samples PbTe was purposely doped with elements other than lead or tellurium to produce either p- or n-type conduction depending on the dopant. Chlorine and bromine were used to convert the samples to n-type and sodium to convert to p-type. The carrier concentration ranged from

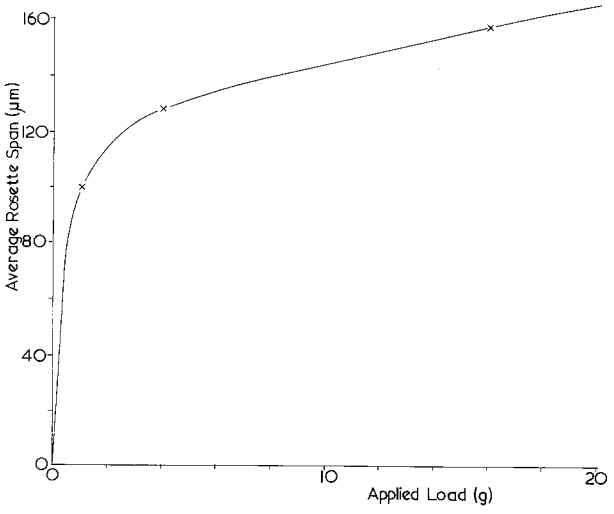

Figure 2 Rosette size as a function of indentor load for p-type PbTe $p \sim 5 \times 10^{17}$ cm^{-3}.

$p = 2.4 \times 10^{19}$ cm^{-3} to $n = 2 \times 10^{19}$ cm^{-3}. The samples measured are presented in Table I.

Figs. 3 and 4 are microhardness versus load for the heavily doped p- and n-type samples respectively and Fig. 5 shows rosette size versus load for both these samples. Alloys of PbTe with SnTe and CdTe, some containing Na as a p-type dopant were measured and the results shown in Fig. 8 and Table I.

6. Results and discussion

6.1. Rosette structure

A typical dislocation pattern associated with indentation under a 2 g load on a (1 0 0) face is shown in Fig. 6. The rosette has four wings parallel to the ⟨1 0 0⟩ directions. It consists of a series of square pyramidal etch pits whose sides are parallel to the ⟨1 0 0⟩ directions. The orientation of the rosettes was found to be independent of the indentor orientation, identically orientated rosettes being produced when the specimen was rotated 45° with respect to the indentor. The average span of the rosette wings in Fig. 6 is 183 μm.

On removal of the surface layer by chemical polishing, the etch pattern was found to have wings of the same width but shorter. Further chemical polishing followed by dislocation etching showed the wings continued to shorten until only a square prism, situated directly beneath the point of indentation, remained. Further polishing was impossible as the sample was required for electrical measurements. However, the structure of the rosette appeared to be identical to those investigated by other workers [8, 9].

The size of the dislocation rosette depended the load (see Figs. 2 and 5). With small applied loads, the rosettes had short rays, each ray having a tendency to form two parallel branches. The opposite branches in a ray are formed by dislocations of different signs and confines a region,

TABLE I

Sample no.	Composition	Dopant	Type	Carrier concentration (cm^{-3})	Symbol in Fig. 8
1	PbTe	Te	p	5×10^{17}	×
2	$Pb_{0.97}Cd_{0.03}Te$	Te	p	6×10^{17}	○
3	$Pb_{0.97}Cd_{0.03}Te$	Te	p	1.2×10^{18}	△
4	$Pb_{0.97}Cd_{0.03}Te$	Na	p	2×10^{19}	●
5	PbTe	Na	p	2×10^{19}	⊙
6	PbTe	Na	p	2.4×10^{19}	□
7	PbTe	Pb	n	1×10^{18}	*
8	PbTe	Cl	n	1.6×10^{19}	△
9	PbTe	Br	n	2×10^{19}	⊗
10	$Pb_{0.99}Sn_{0.01}Te$	Na	p	7×10^{19}	■
11	$Pb_{0.97}Sn_{0.03}Te$	Na	p	8×10^{18}	▽
12	$Pb_{0.97}Sn_{0.03}Te$	Te	p	2×10^{18}	▼

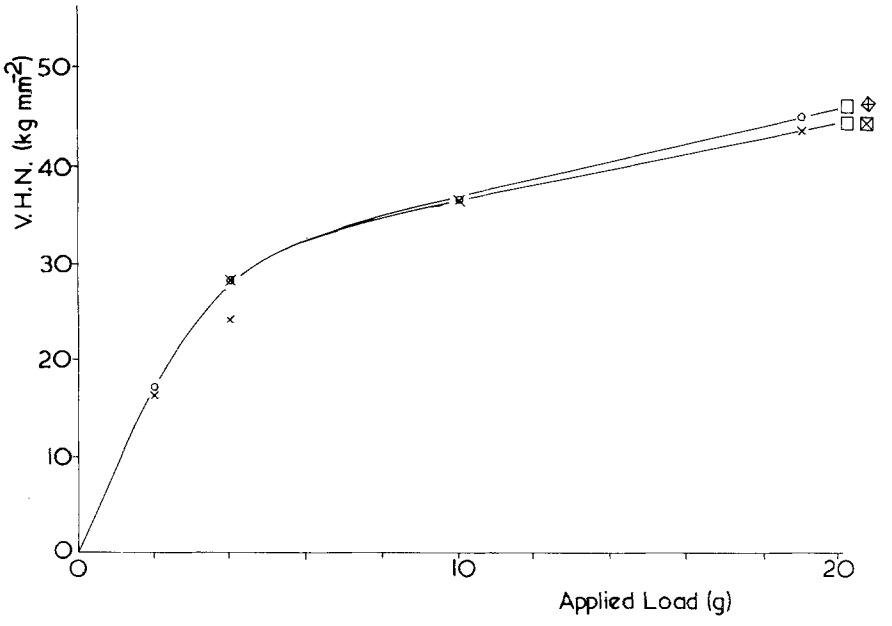

Figure 3 Vickers hardness number as a function of applied load for Na-doped PbTe p ~ 2 × 10^{19} cm^{-3}.□⊠, □⊕ as in Fig. 1.

within which the material has moved tangentially, relative to the surrounding material. Generally, the tendency to form parallel branches was restricted to the ends of each ray (Fig. 6). For cadmium-doped PbTe the effect of splitting into branches was more pronounced.

For ionic crystals which have the NaCl structure, slip occurs in the ⟨1 1 0⟩ (1 1 0) [10, 11]. However, with decreasing ionic nature slip along the (1 0 0) plane becomes more probable [1]. PbTe, which is not very ionic in nature [1] was expected to have a primary glide system (1 0 0) ⟨1 1 0⟩.

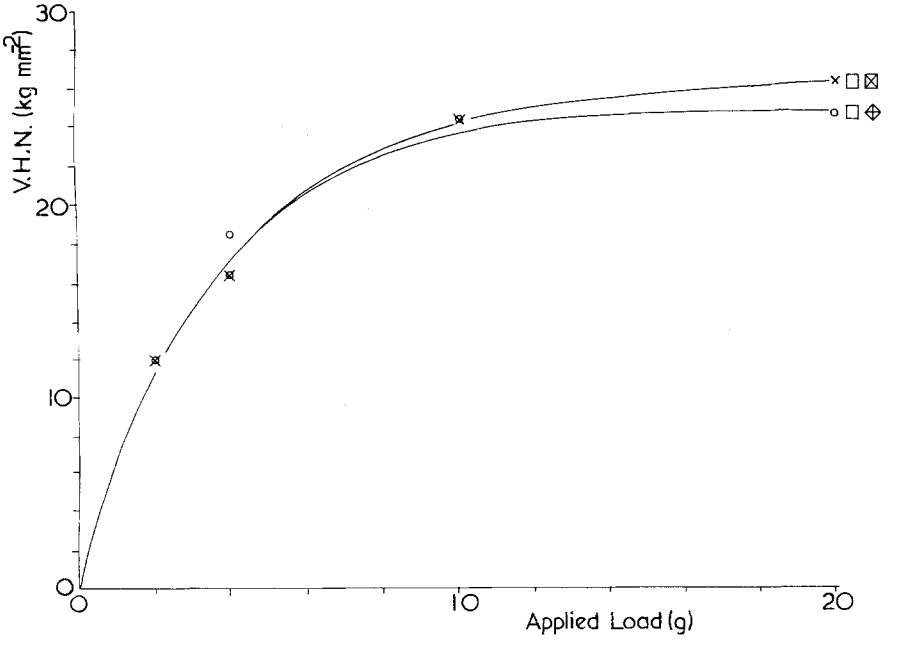

Figure 4 Vickers hardness number as a function of applied load for Cl-doped PbTe n ~ 1.6 × 10^{19} cm^{-3}.

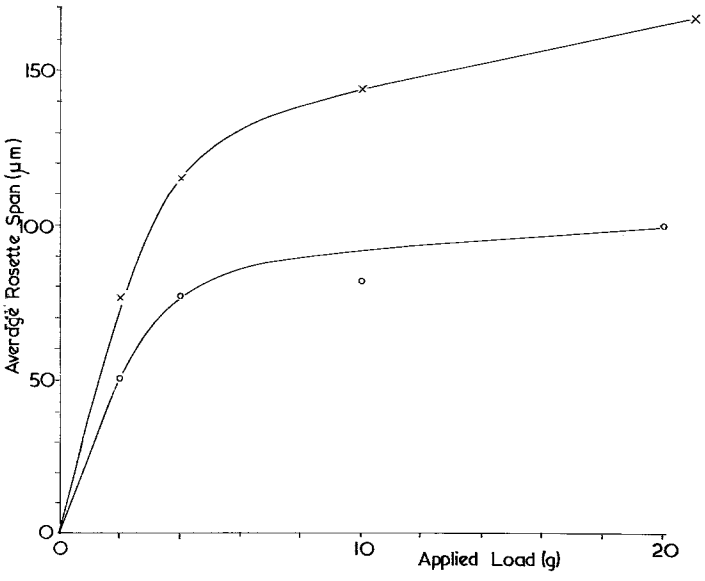

Figure 5 Variation of rosette size as a function of indentor load for PbTe. X: $n \sim 1.6 \times 10^{19}$ cm^{-3} and ○: $p \sim 2 \times 10^{19}$ cm^{-3}.

6.2. Hardness

6.2.1. Undoped PbTe

It can be seen from Fig. 1 that the hardness of the material/unit load decreases quite appreciably with increasing load. The rosette span shows a similar trend although the results were not as accurate.

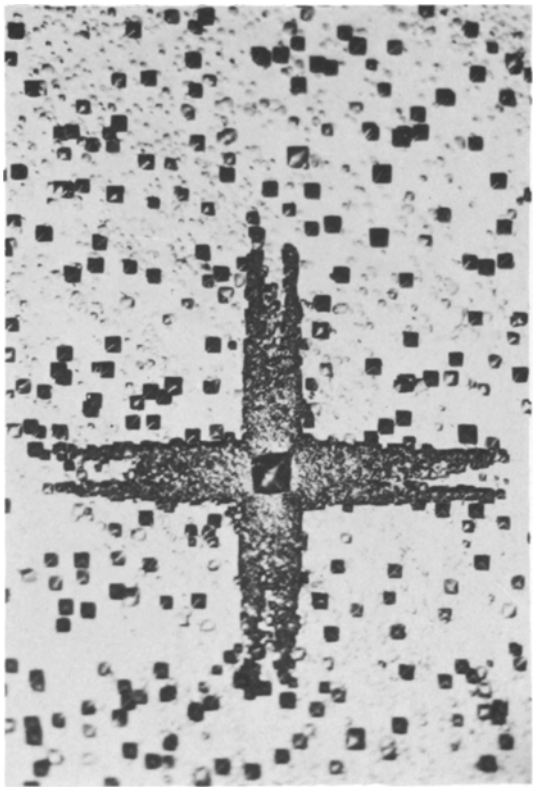

Figure 6 Typical rosette pattern of etch pits showing regions of dislocations after indentation.

The reason for missing the 2 g and 8 g points was because of the large degree of scatter in rosette size. Each point on the graphs is an average of at least three impressions.

In an attempt to produce a possible equation for the hardness versus load curve a graph of $\log_{10}$ hardness was plotted against $\log_{10}$ load, see Fig. 7. The resulting straight lines are of gradient $n = \frac{1}{2}$ with intercepts on the $\log H$ axis equal to $\log k$, i.e.

$$H = k \cdot L^{1/2}.$$

for $p < 10^{18}$ cm^{-3} PbTe, $k \sim 6$ and for $p \sim 2 \times 10^{19}$ cm^{-3} PbTe, $k \sim 11$.

6.2.2. Impurity doped PbTe

Examination of Figs. 3 and 4 shows that hardening also occurs in impurity doped PbTe. The results for heavily doped p-type PbTe are shown in Fig. 8 and it can be seen that this curve is of the same form as that for undoped PbTe. From the dislocation theory one would expect doped PbTe to be harder than undoped PbTe. This is because the introduction into the lattice of impurities ought to cause elastic interaction between dislocations and the impurities. It has been shown [2] that the elastic interaction is dependant, amongst other things, on the quantity $(r_1 - r_0)/r_0$ where r_0 is the radius of the host and r_1 is the radius of the dopant. Ablova *et al.* [2], assuming substitution of the impurity and using covalent octahedral radii, showed that there should be elastic interaction between the impurity atoms and the dislocations for both n- and p-type dopants.

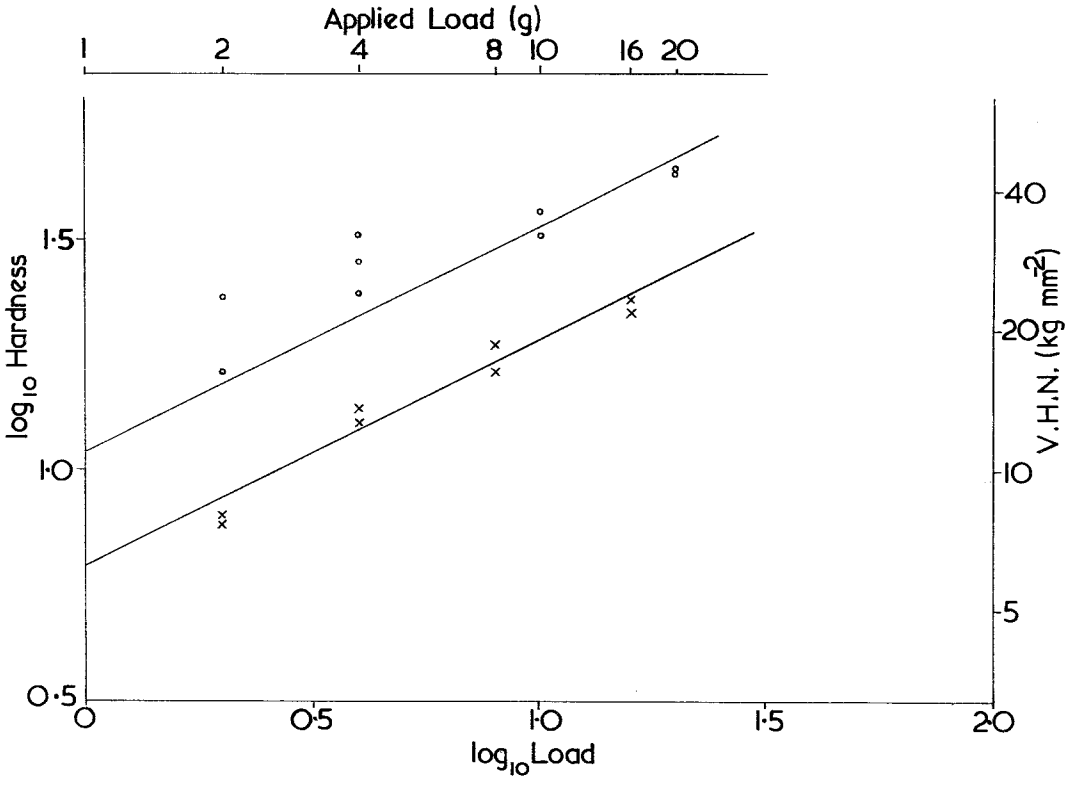

Figure 7 Logarithmic relationship between hardness and load.

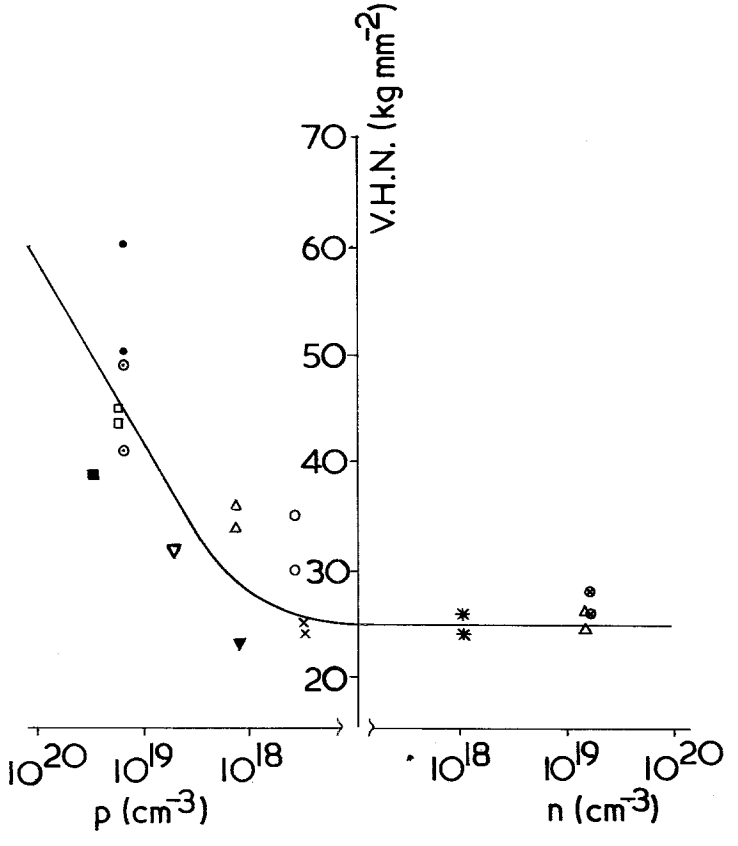

Figure 8 Vickers hardness number as a function of carrier concentration and composition.

This leads to the conclusion that hardening should occur for undoped PbTe whether p- or n-type. However, the difference in hardness between undoped and heavily doped p-type, and the lack of difference between undoped and heavily doped n-type PbTe cannot be explained by the elastic interaction between dislocations and the impurities.

6.4. Effect of large load

The rosette shape for a 50 g load, with the indentor parallel to and at 45° to the (1 0 0) is basically the same as at lower loads although there appears to be less tendency for ray branching. It has been shown [9] by prismatic punching experiments that lead sulphide has a secondary slip system of (1 1 0) ⟨1 1 0⟩ in addition to the (1 0 0) ⟨1 1 0⟩ system usually preferred. No evidence of this secondary slip system was observed for PbTe using a 50 g load.

6.5. Effect of donor and acceptor impurities

The results obtained for mocrohardness determination at 20 g loads are shown in Fig. 8. A similar curve is produced at any other constant load. Again, the results shown for the microhardness are average values.

Before discussion of the results, the principal reasons for the scatter shown in the hardness values were:

(i) the different concentration of dislocations present in the original samples. These are produced by imperfect growth,

(ii) the different concentrations of dislocations introduced during cleavage. After cleaving the number of dislocations present on the surface was approximately 10^5 to 10^6 cm^{-2},

(iii) the anisotropy in the plastic properties of PbTe, which expressed itself by a slight distortion in the shape of the impression.

It can be seen from Fig. 8 that for n-type PbTe the microhardness within its scatter range remains constant throughout the concentration region investigated. For the p-type, the samples with a carrier concentration less than 10^{18} cm^{-3}, had a microhardness equal to that of n-PbTe. With hole concentrations greater than 10^{18} cm^{-3} the microhardness sharply increases. The average microhardness value for the material closest to stoichiometry, i.e. n, p less than 10^{18} cm^{-3}, is 27 ± 1 kg mm^{-2}. When compared to this value, the microhardness of heavily doped p-type PbTe increases approximately 100%. These results are in good agreement with other workers [2].

As discussed earlier, the introduction of impurities into the lattice ought to cause strengthening if the mechanism of elastic interaction between the dislocations and the impurities prevails. By measuring the microhardness of samples with a different impurity present a possible divergence in the respective curves was expected. Since the hardness is practically independent of the concentration of free electrons in the n-type material, and yet very dependent on the concentration of holes in the p-type material, it would appear that this behaviour results from a possible electrostatic interaction between the dislocations and the impurity ions rather than a simple elastic interaction.

It is well known [12] that dislocations in elemental and compound semiconductors may be electrically charged, e.g. edge dislocations in germanium may act as electron acceptors. In an attempt to explain hardening by electrostatic interaction of charged dislocations the following assumptions will be made in order to simplify matters:

(i) the charged dislocations have the same sign

(ii) electrostatic interaction predominates over any elastic interaction. (This is a reasonable assumption considering the concentration of impurities involved).

Consider pure, non-stoichiometric, p-type PbTe where $p \sim 10^{18}$ cm^{-3}. If the non-stoichiometry is increased such that $p > 10^{18}$ cm^{-3} an increase in hardening results. If the non-stoichiometry is decreased, i.e. $p < 10^{18}$ cm^{-3}, the hardness remains unchanged. The only variables in this case are (i) the number of excess Te atoms and consequently (ii) the number of Pb vacancies. Therefore the hardness would appear to be dependent on the number of excess Te atoms and/or the number of Pb vacancies.

If PbTe is doped heavily p-type by the substitution of sodium ions the number of lead vacancies present will be less than in slightly p-type non-stoichiometric PbTe. For non-stoichiometric p-type PbTe one can write a neutrality condition $p = V'_{Pb}$ but for heavily doped p-type one has to consider the following:

$$V^{x}_{Pb} \rightarrow V'_{Pb} + h, \quad \text{i.e. } [V'_{Pb}]\, p = k_1$$

and the neutrality condition

$$p = [Na]$$

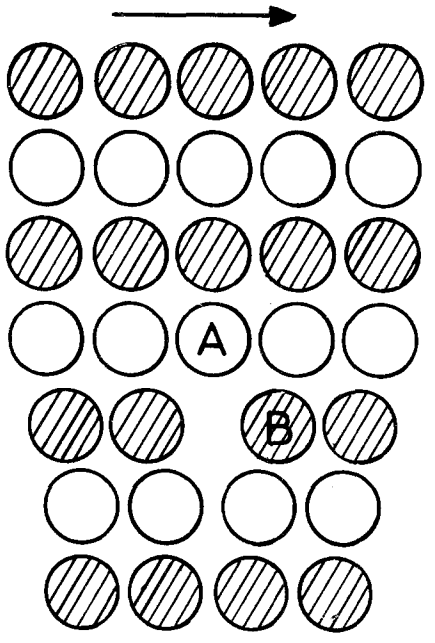

Figure 9 Arrangement of atoms in an edge dislocation for a Burgers vector $\frac{1}{2}$ (1 0 0) ⟨1 1 0⟩ The movement of this dislocation to the right is discussed in the text.

hence:

$$[V'_{Pb}] = k_1/[Na]$$

Here the hardness increases and, since the number of Pb vacancies are less than before, the hardness appears to be due to the substituted acceptor ions.

This leads to the conclusion that the hardness in p-PbTe is dependent on the presence of Pb vacancies and/or acceptor impurities. Since the effect on the hardness by these is similar the interaction between the Pb vacancies, acceptor impurities and the charged dislocations must be similar.

For an edge dislocation in an NaCl lattice with a Burger's vertor $\frac{1}{2}$ (1 0 0) ⟨1 1 0⟩ the arrangement of atoms looks like Fig. 9. The extra half plane terminates with the same type of atom all along its length i.e. either all Pb or all Te. If one considers PbTe to be partially ionic i.e. Pb atoms are charged $\delta +$ and Te atoms $\delta - (\delta < 1)$, then if the terminal atom A in Fig. 9 is Te it will be charged $\delta -$ and atom B will be charged $\delta +$ for stoichiometric PbTe. However, if atom B is a donor atom it will be charged $(\delta + 1) +$ and if it is an acceptor it will be charged $(\delta - 1) +$. For non-stoichiometric p-type PbTe the region of the lead vacancy will be negatively charged, $(1 - \delta) -$ with respect to the lattice. Hence for both non-stoichiometric and doped p-type material the Te atom charged $\delta -$ will have to traverse a position charged $(1 - \delta) -$ if it wishes to move to the right in Fig. 9. This will probably be energetically less favourable than if atom B were charged $\delta +$, as for stoichiometric PbTe, i.e. hardening has occurred. For n-type material no such reduction in attraction occurs. Thus this may be a mechanism whereby electrostatic effects play a more prominent part in dislocation movement.

If one considers the case of the extra half planes terminating in Pb δ^+ the reverse happens, i.e. n-type material should be harder and p-type softer – the reverse of what is actually found.

From Fig. 8 it can be seen that alloying PbTe with CdTe produces hardening and alloying with SnTe produces softening when compared with PbTe samples of equal carrier concentrations. At first sight this would appear to contradict the results of Reli *et al.* [13] and Wagner *et al.* [14] who found, for the PbTe–SnTe system, that hardness increased with increasing SnTe content. However, their curves took no account of the carrier concentration. As SnTe is alloyed with PbTe the psuedo binary existence region of the alloy moves towards the p-type excess Te side, i.e. the n-side shrinks and the p-side expands [15] with a consequent increase in hole concentration [14]. Hence an increase in hardness is expected from this incease in hole concentration but this increase is less than would have occurred for PbTe with a similar carrier concentration. This may be explained by the fact that CdTe increases [3] and SnTe reduces [4] the energy gap when alloyed with PbTe. As a general rule in a semiconductor series as the forbidden energy gap increases the melting point and the bond strengths increase. Hence one would expect that the energy required to move a dislocation would increase as the energy gap (and hence bond strength) increased.

Conclusion

The rosette shape in PbTe has been determined and it has been shown that its three-dimensional geometry and structure is the same as rosettes produced in PbS. The basic shape and orientation of the rosettes is unaffected by either a large load or different orientations of the indentor. The primary slip system has been verified as (1 0 0) ⟨1 1 0⟩.

It has been shown that non-stoichiometric and impurity doped PbTe work hardens. An equation

for the work hardening curve is $H = k \cdot L^{1/2}$ where H = microhardness ($kg\,mm^{-2}$) and L = applied load (g).

The microhardness measured in the dark was found to be no different from that measured in the light. However, the microhardness is not independent of the number of free carriers. Average microhardness for PbTe for the material closest to stoichiometry, i.e. $n, p \sim 10^{18}\ cm^{-3}$, is $27\ kg\,mm^{-2}$. It has been shown that the microhardness is very dependent on the hole concentration when $p > 1018\ cm^{-3}$, the hardness increasing approximately 100% with heavily doped p-type PbTe. It has also been shown that the hardness is independent of the electron concentration, the hardness remaining constant throughout the n-type region.

A possible cause involving the electrostatic interaction of charged dislocations with acceptor impurities and negatively charged vacancies has been discussed.

It was found that CdTe hardened and SnTe softened PbTe. It is suggested that the change in energy gap and hence probable change in bond strength might account for the change in hardness.

Acknowledgements

The authors are grateful for Mr T. Brewer in preparing the drawings and to the referee for his helpful comments.

References

1. M. S. ABLOVA, M. N. KARKLINA and M. N. VINOGRADOVA, *Sov. Phys. Solid State* **11** (1970) 2089.
2. M. S. ABLOVA, M. N. VINOGRADOVA and M. N. KARKLINA, *ibid* **10** (1969) 2089.
3. P. M. NIKOLIC, *Brit. J. Appl. Phys.* **17** (1966) 341.
4. J. DIMMOCK, I. MELNGAILIS and A. J. STRAUSS, *Phys. Rev. Lett.* **16** (1966) 1193.
5. D. G. COATES and W. D. LAWSON, *J. Electrochem. Soc.* **108** (1961) 1038.
6. L. J. van der PAUW, *Philips Res. Reports* **13** (1958) 1.
7. Unpublished work of Zenith Radio Research Corporation (UK) Ltd.
8. A. A. URUSOVSKAYA, R. TYAAGARADZHAN and M. V. KLASSEN-NEKLYNDOVA, *Sov. Phys. Cryst.* **8** (1964) 501.
9. M. S. SELTZER, *J. Appl. Phys.* **37** (1966) 4780.
10. M. J. BUERGER, *Amer. Mineral* **13** (1928) 1.
11. J. J. GILMAN, "Micromechanics of flow in solids" (McGraw–Hill, New York, 1969)
12. H. ALEXANDER and P. HAASEN, *Solid State Physics* **22** (1968) 27.
13. A. M. RELI, A. K. JENA and M. B. BEVER, *Trans AIME* **242** (1968) 371.
14. J. WAGNER and R. K. WILLIARDSON, *ibid* **242** (1968) 366.
15. T. C. HARMAN, *J. Nonmetals* **1** (1973) 183.

Recieved 29 October 1976 and accepted 30 August 1977.